Hydrology
2023; 11(4): 67-84
http://www.sciencepublishinggroup.com/j/hyd
doi: 10.11648/j.hyd.20231104.12
ISSN: 2330-7609 (Print); ISSN: 2330-7617 (Online)

Analysis of Electrical Resistivity Survey Data for Aquifer Potential and Protective Capacity at Mararaba Dan-Daudu Minna, North Central Nigeria

Alfa Idris Alhaji[1], Salako Kazeem Adeyinka[2], Rafiu Abdulwaheed Adewuyi[2], Udensi Emmanuel Emeka[2], Adetona Abbas Adebayo[2, *], Jamilu Shehu[2]

[1]Department of Physics, School of Sciences, Niger State College of Education, Minna, Nigeria

[2]Department of Geophysics, School of Physical Sciences, Federal University of Technology, Minna, Nigeria

Email address:

alfaidris207@gmail.com (Alfa Idris Alhaji), a.abbass@futminna.edu.ng (Adetona Abbas Adebayo)

[*]Corresponding author

To cite this article:

Alfa Idris Alhaji, Salako Kazeem Adeyinka, Rafiu Abdulwaheed Adewuyi, Udensi Emmanuel Emeka, Adetona Abbas Adebayo, Jamilu Shehu. Analysis of Electrical Resistivity Survey Data for Aquifer Potential and Protective Capacity at Mararaba Dan-Daudu Minna, North Central Nigeria. *Hydrology*. Vol. 11, No. 4, 2023, pp. 67-84. doi: 10.11648/j.hyd.20231104.12

Received: September 20, 2023; **Accepted**: October 10, 2023; **Published**: October 28, 2023

Abstract: It is a fact that basement complex regions lacks sufficient overburden that can host sustainable water table, water bearing fractured/weathered rocks referred to as aquifers are usually identified via suitable geophysical methods to proffer solution to water challenges within these regions. This current study targets the exploration of groundwater potential within the Mararaba Dan-daudu community, a suburb of Minna metropolis. Electrical resistivity method was employed to delineate aquifer prospects and their protective capacity within the area of study. The data from thirty-six Vertical Electrical Sounding (VES) survey points were acquired and analysed. Survey points were aligned along six profiles (A – F) with six VES points per profile. Interpretation of VES points along profiles was helpful in determining the number of layers and thickness. The analysis revealed mainly three layers comprising of sand and fresh laterite at the first layer, fractured/weathered basement at the second layer and fresh basement at the third layer. Iso-resistivity mapping was also done at various depths (surface, 5 m, 10 m, 15 m, 20 m, 30 m and 40 m) respectively to investigate the lateral variations of resistivity over a horizontal plane. These showcased the electrical conductance sliced at the depths of interest. Thirteen VES points (A1, A5, A6, B1, B3, B6, C6, D6, E6, F1, F2, F4 and F5) were mapped as having good prospective aquifer properties. Longitudinal conductance was computed for the outlined VES points to determine their Aquifer Protective Capacity (APC). The result of (APC) rating for the 13 VES revealed the frequency and percentage of APC ranged as: 2 VES locations (15.4%) have good APC, 8 VES locations (61.5%) have moderate APC and 3 VES location (23.1%) have weak APC. with only 3 VES locations out of 13 VES locations in the study area revealed weak APC, the results proved that the groundwater potential of the study area has moderately good APC.

Keywords: Aquifer, Electrical Resistivity, Fractured Basement, Vertical Electrical Sounding, Groundwater

1. Introduction

Water is an essential commodity to mankind and it could be found everywhere in the earth's ecosystem. However the water, which exists in such abundance on the earth, is subject to season. time, space and circulation [5]. The search for groundwater has become quite intense in human history. This is due to the fact that government is unable to meet the ever-increasing water demand; inhabitants have had to look for alternative sources such as streams, shallow wells and boreholes. The amount of surface water available for domestic, industrial and agricultural use is insufficient to fulfil the current demand in the world [40, 41]. The search for sustainable, clean and portable water is of vital importance as it aids in the growth of any community [1, 3, 30, 39].

In the historical past, when there is no visible flow of water along the rivers, people used to dig small pits, in the river alluvium, wait and collect the groundwater coming

through seepage and use it for their drinking purposes and for meeting the domestic needs. More than 60 percent of the global population thrives by using only the groundwater resources. Observation shows that groundwater comes from precipitation such as rain, snow, sheet and hail that soak into the ground and become the groundwater responsible for the spring, wells and boreholes [27]. The shallow depth groundwater has been greatly depleted due to over extraction. Groundwater in the form of aquifer is available in different proportions, in various rock types and at various depths, of the earth. In basement terranes where the water table is not easily accessible, exploration of water bearing rocks (aquifers) becomes the alternative to solving water supply challenges [11, 38].

Two tertiary institutions are proposed for the area in which one (Teachers Training Institute) has taken off. Outside the Mararaban Dan-Daudu several isolated settlements are scattered across the vicinity. A major challenge to these communities which could become adverse in future is the availability of clean and potable water for domestic use. It would be essential to have a futuristic approach to this problem.

The study area is the proposed permanent site of new Niger state college of education, which is expected to accommodate large number of students, teaching and non-teaching staff of the college meaning there may be need for properly harnessed sources of water supply. This study is focused on evaluating the groundwater potential on the area using Resistivity method.

2. Location and Geology of the Study Area

The study area Mararaba Dan-Daudu, is strategically/geographically located at an inter section between the road that traverse from Kuta – Gwada – Dandaudu - Kafin Koro – Kwakuti – Abuja and that from Minna Dan-Daudu – Sarkin Pawa to Kaduna. It is a town strategically located for future development, hence most of these towns host markets for foods stuff to the Southern part of the country. It is approximately on longitude $6^0 49^{'} 44.4^{''}$ E and $6^0 50^{'} 37.50^{''}$ E and latitude $9^0 42^{'}$ N and $9^0 42^{'} 49.25^{''}$ N (Figure 1). Within the area are located two other communities that will benefit from the outcome of this research.

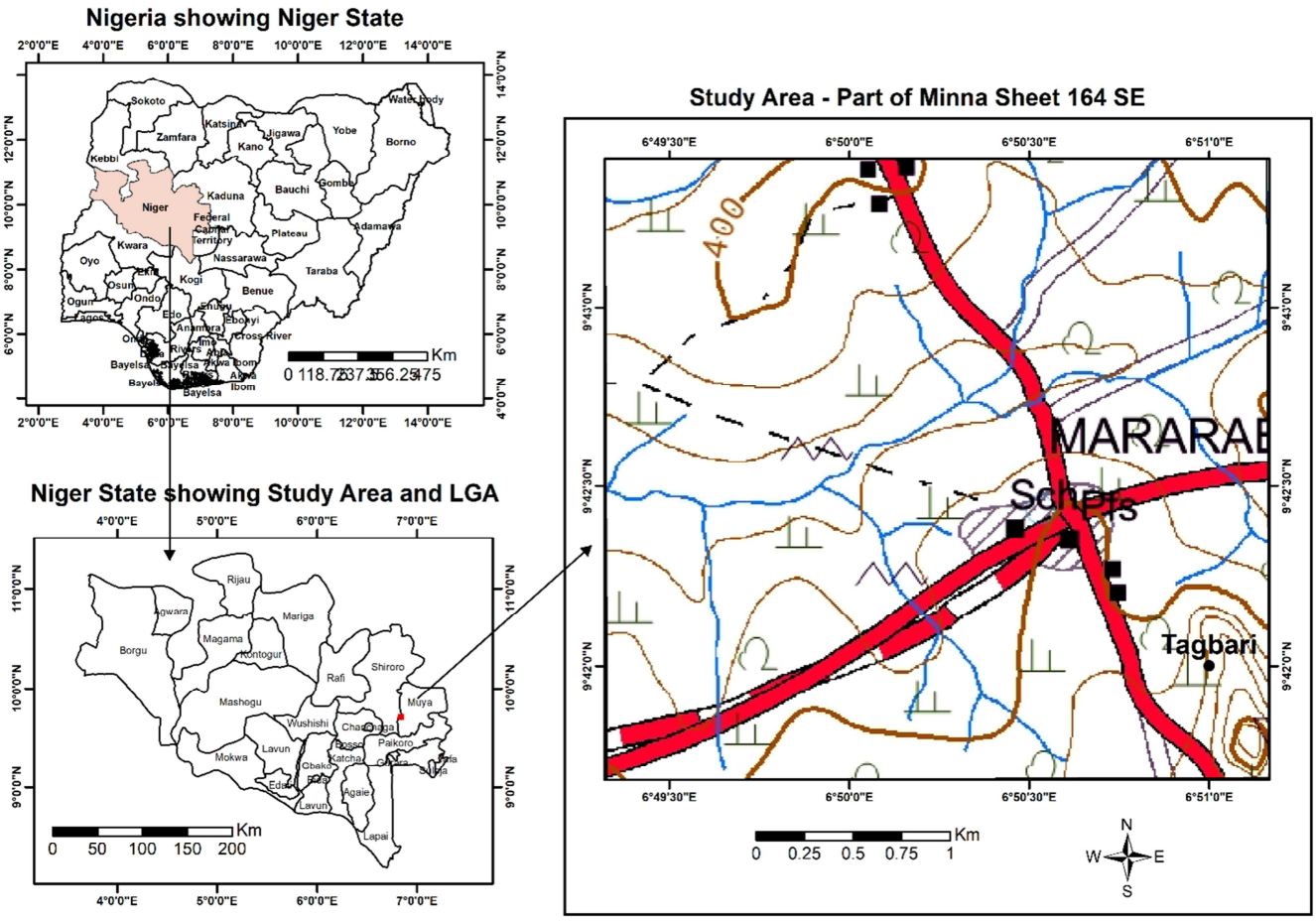

Figure 1. *Location map of part of Niger state indicating showcasing study area.*

The study area lies within the Basement Complex of Northern Nigeria. The Basement Complex includes all rocks older than the late proterrozoic, [19] and is composed mainly of gneisses, granites, migmatite and some extensive area of

schist, phyllites and Quarzites [29].

This area forms part of Minna granitic formation which consist of meta-sediments and meta-volcanics. These meta-sediments include quartzite, gneisses and the meta-volcanics are granites. Around the northern and central part of this area, the rock types are mainly granites while in the eastern and southern part of the area, cobbles of quartzite are found. Although we can also find pegmatite and quartz vein.

The rock type in this area is made of monolithic rocks of granite origin and it can be grouped into two. The groups are (i) the porphyritic to coarse grained granites and (ii) medium to fine grained granites due to their relative grain size. The rocks are mostly weathered and believed to be part of the older granite suite and are mostly exposed along the river channel.

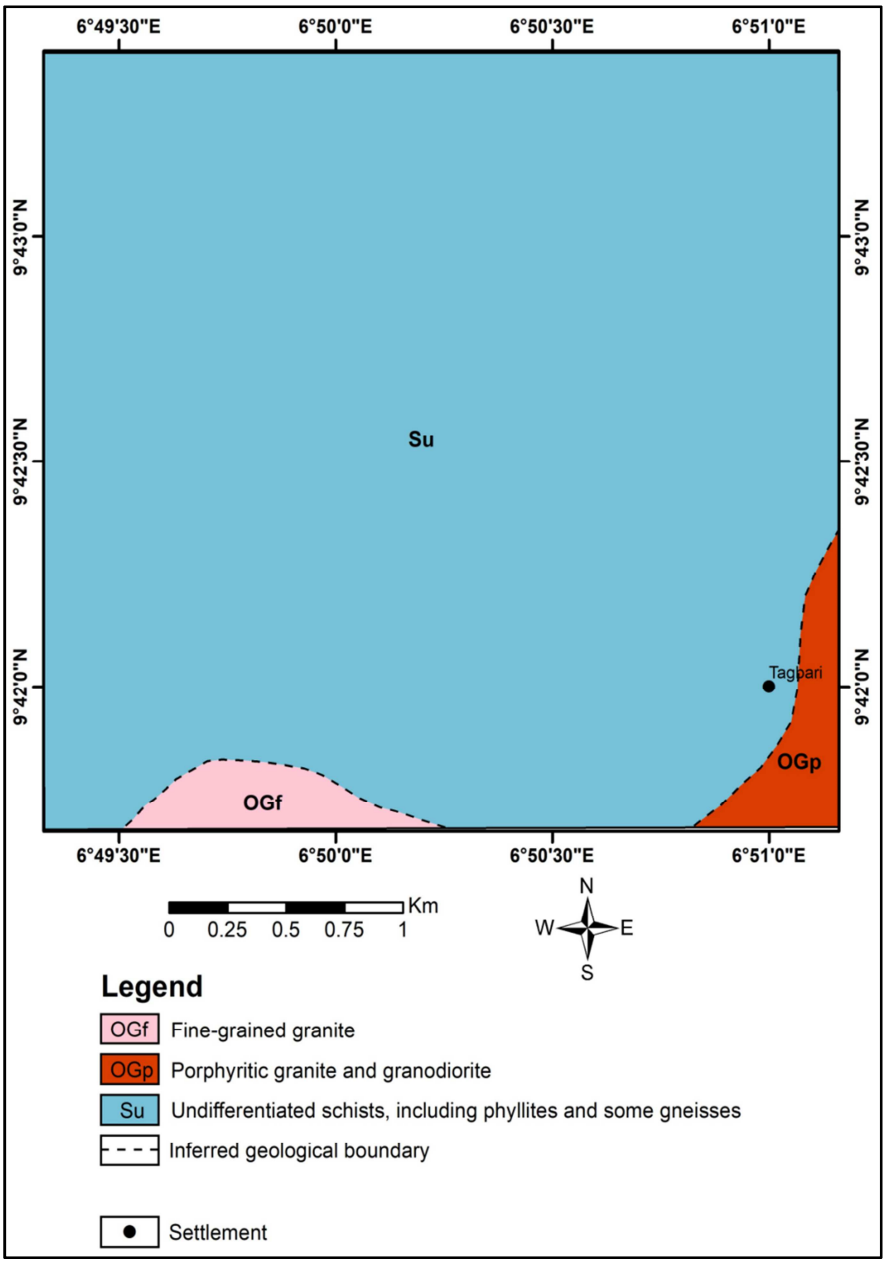

Figure 2. *Geological map of Niger state basement complex and sedimentary basin.*

Porphyritic to coarse grained granite: this granite is referred to as grained granite due to its size and flat lying. They are mostly exposed along the river channels. They range in sizes between few meters to about 80 m. They are most part cut-crossed by the north-south trending quartz and aplitic veins ranging in length 2 m – 15 m. The rocks usually laid in different direction by joints and few most sinistral and dextral faults. Sometimes the outcrops are broken and they are characterised by weathering.

Medium to fine grained granite: the rocks are usually flat lying outcrop exposed along the river channels with a relatively elongated outcrops at the surface. They are less weathered when compared to the ones on the north-south part. They are traverse by east-west trending vein and joints. The

rocks are broken boulders in some parts which shows weathering in form of color change and loose rock fragments [6].

3. Materials and Methods

3.1. Materials

1) *Terrameter*: This is the major instrument used for Electrical Resistivity Survey. The Terrameters used for the data collection were ABEM SAS 4000 and 1000 series.
2) *Electrodes*: These are steel rods of about 30 cm with a base and a pointed end. The pointed end was used to penetrate the ground. Four electrodes were used; the first pair is the potential electrode while the second pair is the current electrode. Their basic function is to pass current into the ground and measure potential between two points.
3) *Cables*: The cables were connected to the terrameter on one end and the other was connected to the electrodes.
4) *Clips*: Used for connecting cables to electrodes. The clips ensure good electrical contact.
5) *Hammer and Cutlass*: Hammer was used to drive the electrodes into the ground.
6) *Tapes*: They were used for marking length to be measured on the field as they have been calibrated in meter (m).
7) *Global Positioning System and Compass-Clinometer*: These were used for taking coordinates and bearing.

3.2. The Theory of Electrical Resistivity Method

This method involves the passage of artificially generated electric current into the earth through the electrodes and in turn causes variation in the subsurface resistivity. This alters the current flow within the earth and also the distribution of electrical potential. The degree of the effect on electric potential is dependent on the size, shape, location and conductivity of the material within the ground. The measurement of electrical potential and current on the earth's surface makes it possible to obtain information about the resistivity variation of the subsurface in the area of interest [36].

The fundamental equation for resistivity survey is derived from Ohm's law [16, 14, 18]:

$$\rho = \frac{RA}{L} \tag{1}$$

where ρ is resistivity, R is resistance, L is length of homogenous conducting cylinder and A is cross sectional area. Water in the soil's pore spaces and the rock's fractures increases the conductivity of the solid earth, which is primarily made of silicates and is therefore essentially a non-conductor. This turns the rock into a semi-conductor when an electrical current is passed through it. Since the earth is not like a straight wire and it is anisotropic, then equation (1) is thus customized to:

$$\rho = \frac{\Delta V}{I}.2\pi r \tag{2}$$

where ΔV is change in voltage and r is the radius of current electrode's small hemisphere.

Since the earth is not homogeneous, equation (2) is used to define an apparent resistivity ρa which is the resistivity the earth would have if it were homogeneous [16]:

$$\rho a = \frac{\Delta V}{I}.2\pi r \tag{3}$$

where 2πr is then defined as a geometrical factor (G) fixed for a given electrode configuration. The Schlumberger configuration was used in this work. The geometric factor G is thus given as:

$$G = \pi \frac{\left[\left(\frac{AB}{2}\right)^2 - \left(\frac{MN}{2}\right)^2\right]}{2\left(\frac{MN}{2}\right)} \tag{4}$$

where AB is (current electrode spacing) and MN is (spacing between potential electrodes).

Schlumberger spread was utilized for the purpose of depth probing, since the potential electrodes are relatively fixed, while the current electrode spacing is expanded symmetrically about the centre of the spread. Schlumberger is less sensitive to undetected lateral variation in resistivity because the potential difference measured between two points is about one third of the electrode spacing. This electrode effect comes to play due to perturbations caused by the passage of potential electrodes over a superficial in homogeneity which is much greater than those due to current electrodes [28, 45]. Since the movement of the potential electrodes are minimised, the electrode movement effect is also minimized thereby enhancing accuracy of measurement.

3.3. Aquifer Protective Capacity (APC)

Aquifer Protective Capacity (APC) simply means the ability of the overburden unit to retard and filter penetrating ground polluting fluid into the aquiferous unit. According to [2, 22], the protective capacity of an aquifer is compared directly with the sum of the longitudinal conductance of all the layers above the aquifer. The protective capacities of identified aquifers in the study area were determined from the longitudinal conductance of the geoelectric layers above the aquifer. This evaluation creates awareness on the state of the aquifers' possibilities to contamination regarding to human activities and industrial discharge [26]. Therefore, the study considered it essential to evaluate the protective capacity of the saturated zone in each location. Aquifer protective capacity, estimates the vulnerability of the underlying aquifer to contamination.

The longitudinal conductance of the overburden layer was obtained using [43] formula:

$$S = \sum_{i=1}^{n} \frac{h_i}{\rho_i} \tag{5}$$

where h = the saturated thickness of each layer

ρ - The layer resistivity

i = Number of layers
S = Longitudinal conductance.

Table 1. *Longitudinal Conductance/Protective Capacity Rating. Modified after [43, 21].*

Longitudinal conductance (mho)	protective capacity rating
>10	excellent
5-10	very good
0.7-4.9	good
0.2-0.69	moderate
0.1-0.19	weak
Below 0.1	poor

4. Analysis and Interpretation of (VES)

The apparent resistivity in ohm-metre determined from the data collected from the thirty-six (36) VES were further analysed as follows:

1) Plotting of resistivity-depth (AB/2) curves for the thirty-six (36) VES points using WinResist version 1.0, (2004) software package for automatic interpretation of Schlumberger sounding.
2) The number of layers, thickness, depth where a layer is starting from and average resistivity values were determined from the resistivity-depth curves.
3) The information determined were summarised in tabular form. (Tables 3, 4; Appendix: Table A1-A4).
4) Geologic sections with their average resistivity values were produced along the profiles using range of resistivity values for various rocks in basement complex (Table 2) compiled by [37, 4, 12] as cited by [13].

Table 2. *Range of Resistivity values for various rock types in Basement complex used in deriving the geologic sections [44].*

Rock type	Range of resistivity (Ωm)
Fadama loam	30-90
Weathered laterite	150-900
Fresh laterite	900-3500
Granite	300-10^5
Clays	1-100
Gravel	100-1500
Alluvium and sand	10-800
Quartzite (various)	10 -2 × 10^8
Weathered laterite	150 – 900
Weathered basement	20 - 500
Fractured basement	500 - 1000
Fresh basement	>1000

4.1. Summary of the VES Results Analysis Along Profile A

General summary of the VES analysis along profile A is as shown in Table 3. There are six (6) VES points on the profile. All the six points have three layers with H curve-type, that is $\rho_1 > \rho_2 < \rho_3$.

The resistivity values for the whole profile ranges from 36.1 Ωm to 4064.3 Ωm. The resistivity values on the first layer ranges from 157.4 Ωm to 3943.8 Ωm and the thickness range between 0.6 m to 3.6 m, the maximum resistivity value on the first layer is at VES station A_6 (3943.8 Ωm) (Fresh Laterite) which is towards the eastern part of the surveyed area, where an outcrop was observed in the field, while minimum value is at VES station A_3 (157.4 Ωm, weathered laterite, Table 2). The resistivity of the second layer range from (36.1 Ωm) A_2 to (89.7 Ωm) A_6 (fadama loam and clay) and the corresponding thickness range between 8.2 m to 33.4 m, the thickest VES point is at A_5 and thinnest is at VES A_4. The low apparent resistivity of second layer maybe due to aquifer presence, especially at VES points A_5 and A_6, where the layer thickness are high. The third layer has resistivity value range from 679.1 Ωm (A_1) to 4064.3 Ωm (A_3). Profile A_6 has the highest first layer apparent resistivity (3943.8 Ωm) while the highest basement apparent resistivity (4064.3 Ωm), was observed at VES A_3. The depth of occurrence of basement along profile A, range from 9.6 m to 33.7 m. VES A_4 has shallowest basement starting from 9.6 m while VES A_5 has the thickest basement starting from 33.7 m and all end at infinity. Except at VES A_1, where basement apparent resistivity value is that of weathered/Fractured layer (679.1 Ωm), the rest resistivity of the third/basement layer are of fresh basement (Table 3).

Table 3. *Summary of VES results analysis along profile A.*

VES point	Type of curve	No of layers	Average resistivity (Ωm)	Layer thickness (m)	Depth starting from (m)
		1	1541.6	3.6	0.0
A_1	H	2	41.2	13.3	3.6
		3	679.1	∞	16.9
		1	648.0	1.4	0.0
A_2	H	2	36.1	9.1	1.4
		3	2555.7	∞	10.5
		1	157.4	0.6	0.0
A_3	H	2	38.0	13.9	0.6
		3	4064.3	∞	26.8
		1	331.4	1.4	0.0
A_4	Ha	2	72.5	8.2	1.4
		3	1196.0	∞	9.6
		1	976.7	1.3	0.0
A_5	H	2	42.0	33.4	1.3
		3	3018.7	∞	34.7
		1	3943.8	1.6	0.0
A_6	H	2	89.7	20.5	1.6
		3	931.2	∞	22.1

4.2. Summary of the VES Results Analysis Along Profile F

There are six (6) VES points on profile F as shown in Table 4 and three distinct layers are prominent on all the VES points, with H curve-Type.

The first layer has a resistivity values range between 66.2 Ωm (alluvium and sand) and 2266.6 Ωm (fresh laterite) and the corresponding thickness is between 0.6 m and 3.8 m. The maximum thickness on the first layer is at VES F_2 (3.8 m) and the minimum thickness is at VES F_2 (0.6 m). The resistivity value of the second layer ranges from 15.8 Ωm (Clay) to 421.8 Ωm (Weathered laterite) and the corresponding thickness range between 17.8 m and 44.5 m. The thickest VES point is at F_4 and the thinnest is at VES point F_3.

Table 4. *Summary of VES Results Analysis along Profile F.*

VES point	Type of curve	No of layers	Average resistivity (Ωm)	Layer thickness (m)	Depth starting from (m)
		1	1039.3	2.5	0.0
F_1	H	2	80.7	28. 7	2.5
		3	4272.9	∞	31.2
		1	1401.3	3.8	0.0
F_2	H	2	105.5	35.4	3.8
		3	1687.1	∞	39.2
		1	2545.7	1.3	0.0
F_3	H	2	421.8	17.7	1.3
		3	11725.6	∞	19.0
		1	2266.6	0.6	0.0
F_4	H	2	172.4	44.5	0.6
		3	882.4	∞	44.5
		1	66.2	1.1	0.0
F_5	H	2	61	30.1	1.1
		3	1414.4	∞	30.1
		1	194.2	1.2	0.0
F_6	H	2	15.8	17.8	1.2
		3	7596.8	∞	17.8

The third layer has resistivity range from 882.4 Ωm (weathered/fractured basement) to 7596.8 Ωm (fresh basement) (Table 4), with infinite thickness. The shallowest depth is at VES F_6 (17.8 m) while the deepest depth is at VES F_4 (44.5 m). The first layer resistivity indicated Clay, Weathered lateritic topsoil. Second layer has resistivity values which correspond with that of fadama loam, clay, alluvium and sand, they have very low resistivity values compared with the resistivity values of first and the third layers.

Table of summary for VES result analysis for profile B to E is appended on appendix (Tables A1-A4).

4.3. General Deductions and Correlations of Iso-Resistivity Contour Maps at Various Depths

The analysis from VES result analysis for profiles makes it much easier to draw a certain number of deductions as regarding the depth and thickness of each layer and zone of water saturation known as (aquifer).

Iso-resistivity maps reflect the lateral variations of resistivity over a horizontal plane at a given depth. In other words, these Iso-resistivity contoured maps indicate resistivity distribution in an area against the distance of current electrodes. This was achieved by plotting the resistivity data corresponding to the depth of interest (picked from the log table) for all the study area. Surfer 13 software version was used to contour these maps which showed the conductivity pattern with depth through the horizontal slicing of the study area. The depths of interest are, the surface, 5 m depth, 10 m depth, 15 m depth, 20 m depth, 30 m depth and 40 m depth. Contour maps for surface, 5 m depth, 10 m depth, 15 m depth, 20 m depth and 30 m depth is presented on appendix (Figure A1-A6).

4.4. Interpretation of Iso-Resistivity Contour Map at 40 m

The Iso-resistivity contour map at 40 m depth was produced as shown in Figure 3, the map was contoured at an interval of 100 Ωm.

The resistivity value ranges from 0 Ωm to 4400 Ωm, the low resistive ($\rho < 600$ Ωm) area still occurred at this depth, which indicate that weathered basement still continued at this depth, areas where this occurred that is, the eastern part of the studied area, and the area where the villagers resides. The low resistivity here maybe as a result of human activities going on there, such as refuse dump.

Areas where the resistivity is that of weathered/fractured basement are very few and they are toward western part. Finally, at the western part of the map, is where the resistivity values are that of fresh basement ($\rho > 1000$ Ωm). A trailing small point with $\rho < 200$ Ωm, that featured at 30 m depth probing, still appeared at the same point at 40 m depth (figure 3); this might be as a result of a conducting mineral at that point, activity of the artisan miners on the studied area also confirmed such, they were notice packing the top sand to go and wash for gold mining. Also, not far from this point, is a very deep hole (more than 16 ft) dug by the artisan miners, for their mining activities.

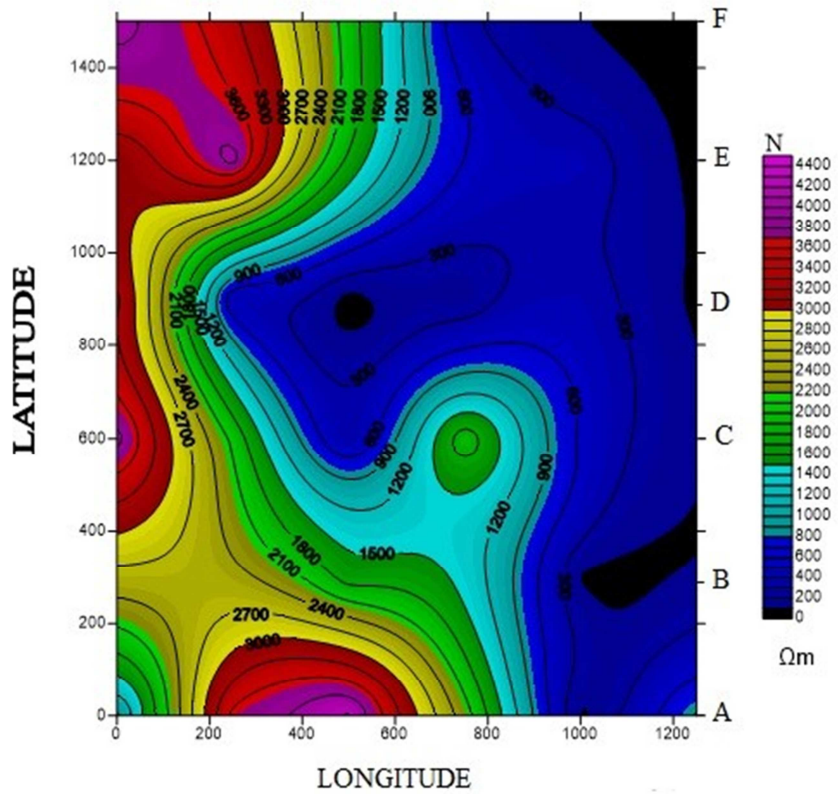

Figure 3. *Iso-Resistivity map at 40 metres, Contour Interval = 100 m.*

4.5. Interpretation of Iso-Resistivity Contour Map for the Second Layer

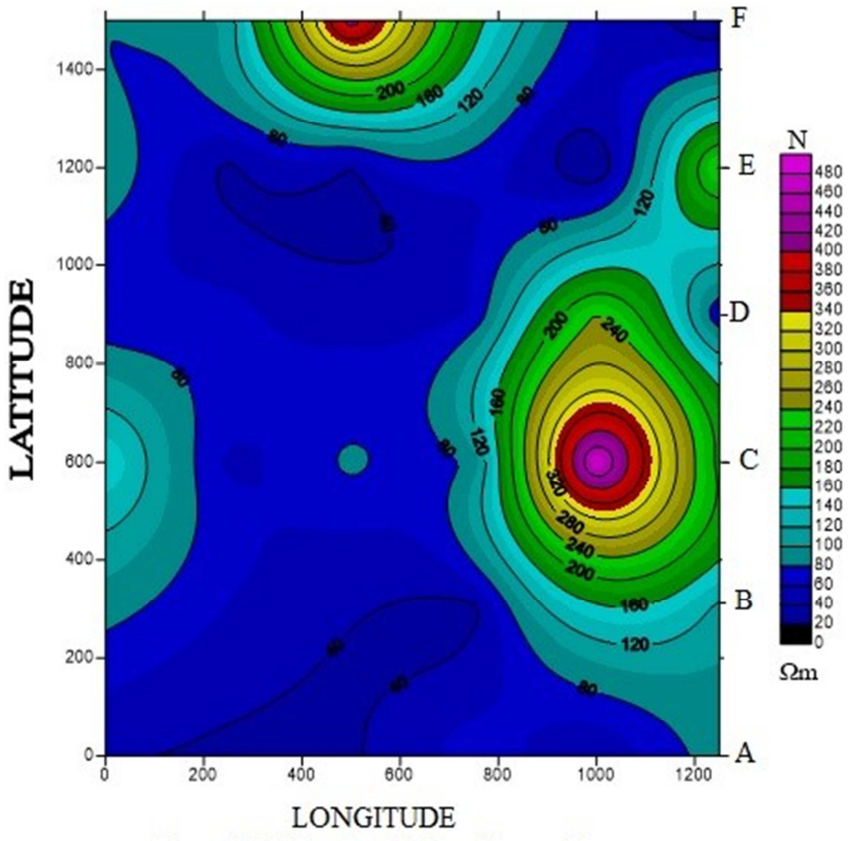

Figure 4. *Iso-Resistivity map of Second Layer, Contour Interval = 20 m.*

The Iso-resistivity contour map of second layer was produced as shown in Figure 4, the map was contoured at an interval of 20 Ωm, the contour lines trend towards North-Western direction.

The resistivity value ranges from 0 Ωm to 480 Ωm. From the map, it is observed that the resistivity value of the whole area is generally low, this may be due to the presence of water and some conductive mineralisation at this layer. The blue colour with apparent resistivity (ρ) which ranges between 20 and 80 Ωm and dominate the entire map has resistivity value which corresponds to the resistivity of clay (Table 2), The areas with yellow, red and brown colours which appear at North central and East central parts of the study area correspond to that of weathered basement.

Comparing trends at 15 m depth (appendix 1d) and entire second layer (Figure 4), it was noticed that they almost have the same value, even where high resistivity closure was noticed on north central of depth 15 m map, Profile F, VES F_3, it was also noticed at the same VES point on figure 4, this implies that second layer was concentrated within 15 m depth of the surveyed area.

4.6. Interpretation of Iso-Resistivity Contour Map for the Third Layer

The Iso-resistivity contour map of the third layer was produced as shown in Figure 5, the map was contoured at an interval of 100 Ωm, the contour lines looks almost parallel in the North-Southern direction while the closures trend North-Eastern direction.

The resistivity value ranges from 400 Ωm to 4800 Ωm. From the map, it is observed that the resistivity value of the whole area is generally high compared with that of second layer. The whole area has resistivity of either Weathered or Fractured or fresh basement. Blue colours has resistivity value which corresponds to the resistivity of Weathered/fractured basement (Table 2).

Comparing trends at 40 m depth (Figure 3) and third layer (Figure 5), it was observed that their contour lines look alike, (parallel) with high resistivity values, at the western part and low resistivity value at the eastern parts of the two figures, this implies also that, third layer resistivity concentrated at the depth of 40 m.

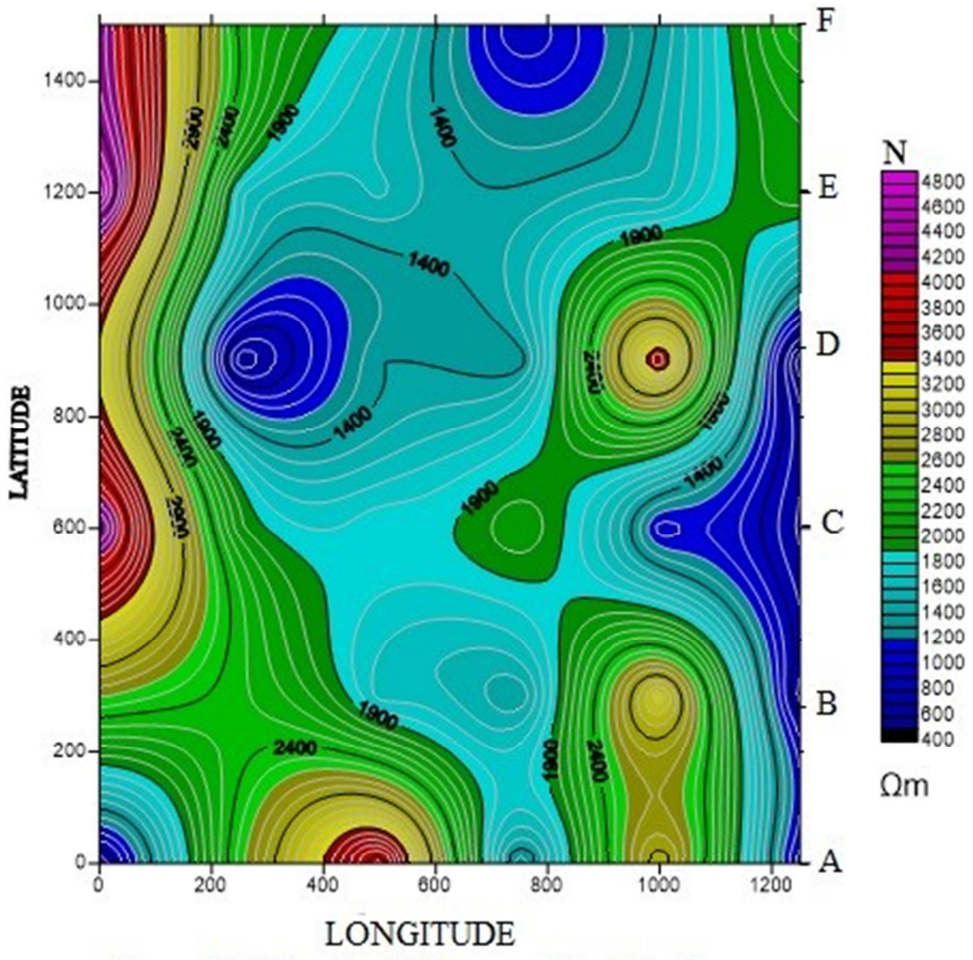

Figure 5. *Iso-Resistivity map of Third Layer, Contour Interval = 100 m.*

The areas with yellow, red and brown colours which appear at all the Western, South central and North-Eastern parts of the study area correspond to that of Fresh basement.

4.7. Interpretation of Contour Map for the Overburden Thickness

Figure 6 is the contour map of the depth to the basement or overburden thickness map, the map was contoured at an interval of 5 m.

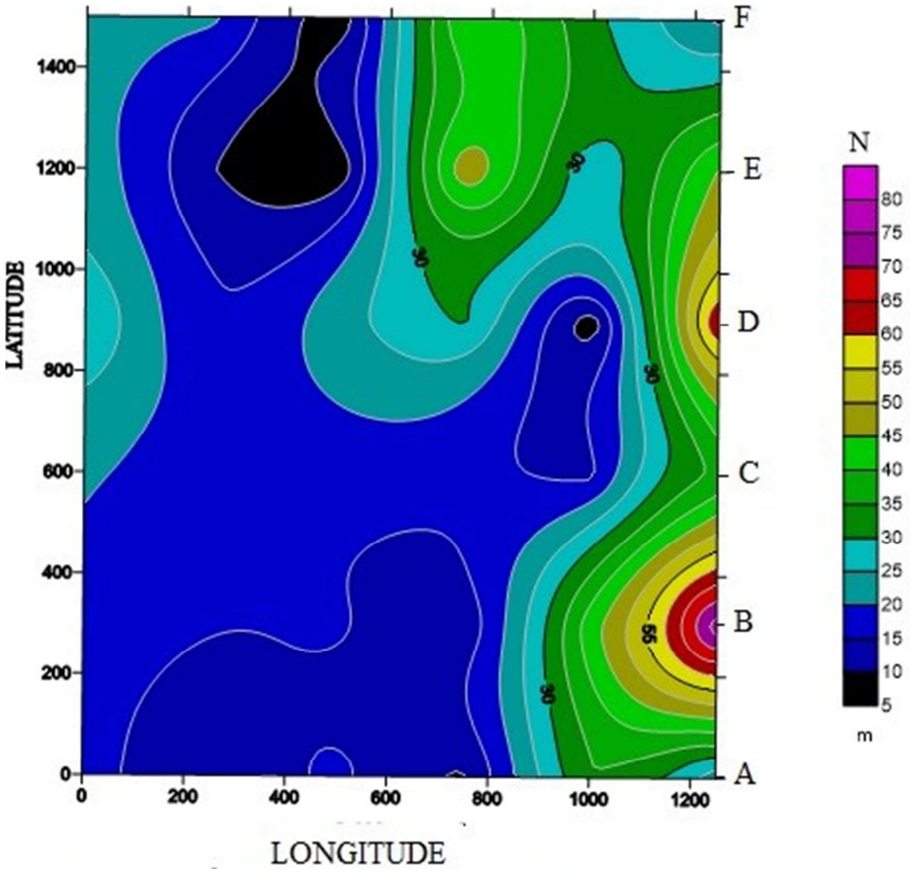

Figure 6. *Contour map of Overburden Thickness, Contour Interval = 5 m.*

The depth ranges from 5 m to 85 m, the depth to basement values used for the contour map corresponds to the depth to the last layer for the whole VES points in the surveyed area. From the map, it was observed that the deepest area was found around the eastern part, Profile B, VES B_6 and Profile D, VES D_6) and the shallowest area is found at Profile E, VES E_5, this may be attributed to the very deep channel washed away by gulley erosion found around that area, which might had washed away the top soil around that point.

Table 5. *Depth to Fresh Basement of the Area, Longitudinal Conductance, Protective Capacity Rating and Curve Type.*

VES Station	Elevation (m)	Depth To Basement (m)	Longitudinal Conductance (mho)	Protective Capacity Rating	Curve Type
A_1	397	16.9	0.40	Moderate	H
A_2	387	10.5	0.29	Moderate	H
A_3	393	26.8	0.71	Good	H
A_4	358	9.6	0.13	Weak	H
A_5	397	34.7	0.80	Good	H
A_6	406	22.1	0.25	Moderate	H
B_1	375	40.1	0.45	Moderate	H
B_2	378	10.1	0.19	Weak	H
B_3	388	39.4	0.10	Weak	H
B_4	408	73.6	0.63	Moderate	H
C_1	389	20.9	0.13	Weak	H
C_2	377	10.1	0.18	Weak	H
C_3	390	17.2	0.20	Moderate	H
C_4	396	14.8	0.11	Weak	H
C_5	391	14.3	0.03	Poor	H
C_6	379	35.9	0.19	Weak	H
D_1	379	21.2	0.33	Moderate	H
D_2	387	15.3	0.22	Moderate	H

VES Station	Elevation (m)	Depth To Basement (m)	Longitudinal Conductance (mho)	Protective Capacity Rating	Curve Type
D_3	405	23.6	0.04	Poor	H
D_4	405	12.2	0.20	Moderate	H
D_5	388	41.2	0.17	Weak	H
D_6	401	65.6	0.11	Weak	H
E_1	379	28.7	0.29	Moderate	H
E_2	382	10.5	0.29	Moderate	H
E_3	381	6.7	0.17	Weak	H
E_4	384	12.4	0.18	Weak	H
E_5	383	5.5	0.30	Moderate	H
E_6	386	45.5	0.19	Weak	H
F_1	389	31.2	0.39	Moderate	H
F_2	390	39.2	0.37	Moderate	H
F_3	383	19.0	0.05	Poor	H
F_4	384	44.5	0.26	Moderate	H
F_5	383	30.1	0.49	Moderate	H
F_6	379	17.8	1.13	Good	H

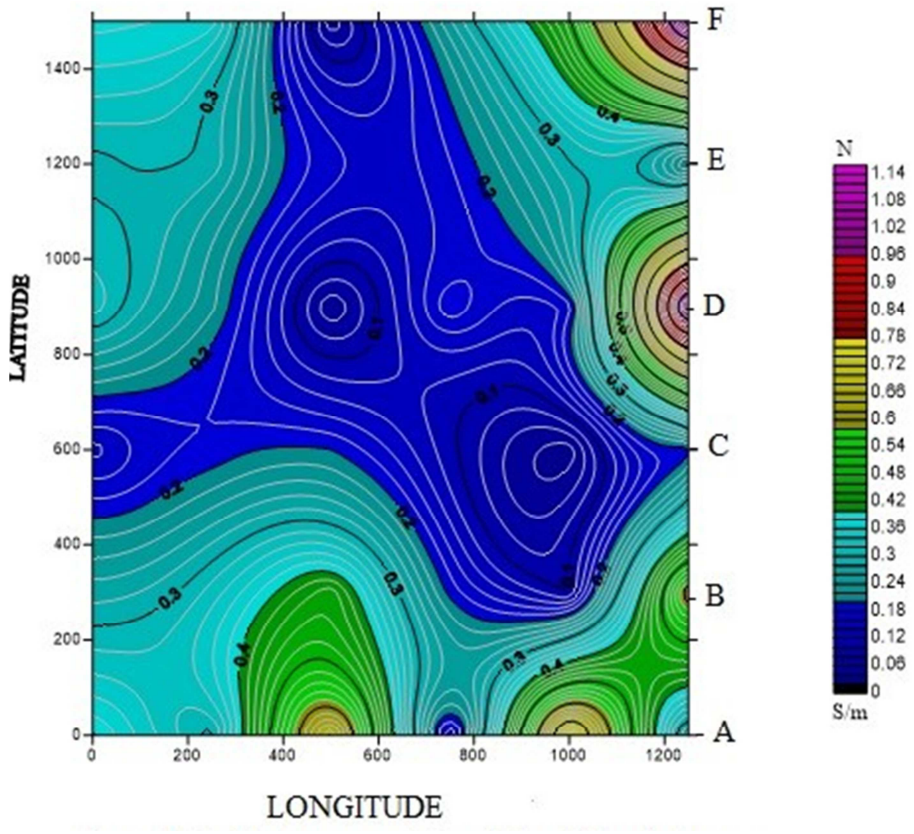

Figure 7. *Contour map of Longitudinal Conductance, Contour Interval = 0.02 S/m.*

From Table 5, it could be seen that the aquifer potentials have poor, weak, moderate and good protective capacities, having a longitudinal conductance ranging from 0.03 mho to 1.13 mho. The longitudinal conductance was calculated using equation 5. The highest longitudinal conductance for the aquifer potential was seen at VES F_6 (1.13) and the lowest was seen at VES C_5 (0.03).

The contour map of longitudinal conductance for the whole study was produce as shown in Figure 7, the map was produced at an interval of 0.02 mho.

The longitudinal conductance ranges from 0 mho to 1.14 mho, with the highest at VES F_6, while the lowest is at VES C_5.

4.8. Aquifer Protective Capacities Evaluation

In a basement complex terrain, areas with overburden thickness of 15 m and above and fractured layer resistivity of 400 Ωm are good for groundwater development [8]. In addition, in basement complex, the areas with low resistivity, thick overburden and fractured bedrock constitute the aquifer units [25, 33, 34]. The author [7, 23] stated that the highest groundwater yield in basement complex is often obtained from a fractured aquifer or a subsurface sequence that has a combination of a significantly thick and sandy weathered layer. In view of above, 13 VES points were delineated as aquifer potentials of the surveyed area, they are as shown in

Table 6.

Table 6. *Aquifer Potential for the Study Area.*

VES Point	Latitude	Longitude	Fractured/Fresh basement Resistivity (Ωm)	Layer Depth Starting From (m)	Longitudinal Conductance (Ohm^{-1})	Protective Capacity Rating
A_1	1073000	262100	679.1	16.9	0.40	Moderate
A_5	1073000	263100	3018.7	34.7	0.80	Good
A_6	1073000	263350	931.2	22.1	0.25	Moderate
B_1	1073300	262100	1653.9	40.1	0.45	Moderate
B_3	1073300	262350	3304.4	39.4	0.10	Weak
B_6	1073300	263350	748.3	73.6	0.63	Moderate
C_6	1073600	263350	676.3	35.9	0.19	Weak
D_6	1073900	263350	502.5	65.6	1.11	Good
E_6	1074200	263150	911.1	45.5	0.19	Weak
F_1	1074500	261900	4272.9	31.2	0.39	Moderate
F_2	1074500	262150	1687.1	39.2	0.37	Moderate
F_4	1074500	262650	882.4	44.5	0.26	Moderate
F_5	1074500	262900	1414.4	30.1	0.49	Moderate

From Table 6, it is shown that the aquifer potentials have weak, moderate and good protective capacities having a longitudinal conductance ranging from 0.10 Ohm^{-1} to 1.11 Ohm^{-1}. The highest longitudinal conductance for the aquifer potential was seen at VES D_6 (1.11 Ohm^{-1}) and the lowest was seen at VES B_3 (0.10 Ohm^{-1}).

According to the aquifer protective capacity (APC) rating of [43, 21], the frequency and percentage of APC are ranged as follows; 2 VES locations (15.4%) have good APC, 8 VES locations (61.5%) have moderate APC and 3 VES location (23.1%) have weak APC (Table 6). These show that only 3 VES locations out of 13 VES locations in the study area revealed weak APC (Figure 7). The impermeable and thick clay overburden materials which are characterized by low hydraulic conductance serve as natural filters to any percolating fluid [31, 42, 15]. These material reduce the rate of movement of the fluid through them hence, increasing their residence time and offering better protection to the underlying aquifers [17].

An effective groundwater protection is provided by protective layers with sufficient thickness and low hydraulic conductivity leading to high rate of percolating water [20]. Areas with high longitudinal conductance (thick overburden and low resistivity) constitute regions of excellent – good aquifer protective capacity in which such locations have sufficient seal from groundwater contamination. Locations with moderate aquifer protective capacity are less susceptible or rare to contamination while areas with weak – poor APC are susceptible to contamination [10]. These results show that the groundwater potential of the study area is moderately good and indefinite locations of weak aquifer protective capacity of the overburden.

In a basement complex terrain, areas with fresh basement layer depth of 4 m and below are good for civil engineering work. [8, 32, 35], stated that, where the overburden layer thickness is thick, such an area is unsuitable for construction of high-rise buildings but very good area for groundwater exploration. They also stated that incompetent zone for erecting of high-rise structures, are zones (shallow/deep fracture) but are better sites for hydrogeological purposes. And the competent zones are the poorly weathered zones which are better sites for erecting of heavy structures.

5. Conclusion

For this research work, Electrical Resistivity data were collected using Vertical Electrical Sounding (VES) using Schlumberger array across all the thirty six (36) VES points, taken along the 6 profiles. This Schlumberger electrode layout was used, because the smaller separation of the potential electrodes reduces noise due to ground current (from cultural and telluric sources) which may limit the useful depth of penetration. Similarly, the maximum current electrode separation of 430 m and potential electrode of 100 m were reached and this corresponds to 215 m probed depth (i.e AB/2), there was no need for data reduction or repeated measurement since the receiver of SAS 4000 discriminates noise and measures voltages corrected with transmitted signal current. The system has the built-in function to average the best measurement of maximum of four staking with the standard deviation of unity or even less [45]. The apparent resistivity data were generated from resistance values, using equation (3) and (4). WIN-resist software was used to interpret the data. This particular software perform automatic interpretation of the Schlumberger sounding curves which then gives the equivalent numbers of n-layer model input from the apparent resistivity data of particular sounding point, which then converts the apparent resistivity as a function of electrode spacing the true resistivity value as a function of depth. The vertical electrical sounding data were interpreted to obtain geo-electric section, geologic section and finally iso-resistivity maps at various depths.

The result obtained show that the area is generally underlain by three geologic formation (lateritic top soil, weathered/fracture basement and fresh basement. With average first layer resistivity of 1065.6 Ωm, with highest value of 3943.8 Ωm at VES A_6 and lowest value of 1331.6 Ωm at VES D_4, the layer also has an average thickness of 1.7 m with highest value of 4.0 m (VES B_4) and lowest value of 0.6 m (VES A_3 & F_4). Second layer has average resistivity

value of 129.5 Ωm with highest value of 556 (D_3) and lowest value of 15.8 Ωm (F_6) with corresponding average thickness of 23.0 m which ranges from 4.1 m VES E_5 to 73.6 m VES B_4. Finally third layer has an average resistivity of 3573.3 Ωm, with least value of 776.3 Ωm and highest value of 22750.7 Ωm with depth averagely starting from 25.6 m, the least depth starting from 5.5 E_5 and deepest value starting from 73.6 m (E_5).

With regard to aquifer protection capacity (APC), only 3 VES locations out of 13 VES locations in the study area that was delineated as aquifer potential, has weak APC (Table 6), (Figure 7). The results proved that the groundwater potential of the study area has moderately good APC; hence the aquifers of the study area constitute definite overburden thickness with clay which serves as natural filter to percolating fluids. The result also showed that the aquifers in the study area have moderate-low vulnerability to contamination because the APC is moderately good, except for only 3 VES points, which have weak APC.

The presence of interconnectivity of fracture zones in the study area showed that the area has good prospects for groundwater development and it can be recommended that the search for groundwater in the study area should be aimed at searching for fractured zones where overburden is relatively thin. Areas that are extensively fractured and where the fractures are deep are considered as weak zones and considered suitable zones for groundwater development [7, 32].

VES analysis revealed three lithologic sequences which include topsoil, weathered layer and fractured or fresh bedrock. H-type are the curve types obtained from the VES data with overburden thickness ranging from 8.2 m to 73.6 m. The bed rock is averagely covered with thick overburden which is unsuitable for construction of heavy structures but would be useful for small scale groundwater exploration [33, 34, 35] such as development of hand-dug well and hand-pump well. The iso-resistivity map of the weathered layer revealed the area is of good groundwater potential but incompetent for engineering structures.

Appendix

Tables A1-A4: Summary of VES results analysis along profile B, C, D and E.

Table A1. *Summary of VES results analysis along profile B.*

VES point	Type of curve	No of layers	Average resistivity (Ωm)	Layer thickness (m)	Depth starting from (m)
		1	209.8	2.1	0.0
B_1	H	2	42.2	13.6	2.1
		3	1653.9	∞	40.1
		1	1564.0	1.3	0.0
B_2	H	2	52.4	10.1	1.3
		3	1395.8	∞	10.1
		1	724	3.3	0.0
B_3	H	2	395.6	39.4	3.3
		3	3304.4	∞	39.4
		1	436.7	4.0	0.0
B_4	H	2	117.5	73.6	4.0
		3	748.3	∞	73.6

Table A2. *Summary of VES results analysis along profile C.*

VES point	Type of curve	No of layers	Average resistivity (Ωm)	Layer thickness (m)	Depth starting from (m)
		1	2126.0	1.5	0.0
C_1	H	2	158.6	19.4	1.5
		3	4483.8	∞	20.9
		1	210.2	0.7	0.0
C_2	H	2	54.7	9.4	0.7
		3	5008.6	∞	10.1
		1	1961.7	1.0	0.0
C_3	H	2	85.7	16.2	1.0
		3	1892.0	∞	17.2
		1	1221.7	1.2	0.0
C_4	H	2	86.7	13.6	1.2
		3	22750.7	∞	14.8
		1	1227.3	1.4	0.0
C_5	H	2	484.2	12.9	1.4
		3	1033.1	∞	14.3
		1	775.2	0.9	0.0
C_6	H	2	190.6	35.0	0.9
		3	676.3	∞	35.9

Table A3. *Summary of VES Results Analysis along Profile D.*

VES point	Type of curve	No of layers	Average resistivity (Ωm)	Layer thickness (m)	Depth starting from (m)
		1	298.4	1.7	0.0
D_1	H	2	63.9	19.5	1.7
		3	12663.2	∞	21.2
		1	571.1	1.3	0.0
D_2	H	2	68.1	14.0	1.3
		3	598.1	∞	15.3
		1	749.2	2.4	0.0
D_3	H	2	556.0	21.2	2.4
		3	1398.9	∞	23.6
		1	1853.5	0.9	0.0
4_D	H	2	62.2	11.3	0.9
		3	1545.1	∞	12.2
		1	1210.0	1.8	0.0
D_5	H	2	242.0	39..4	1.8
		3	8405.0	∞	41.2
		1	1804.3	2.3	0.0
D_6	H	2	59.3	63.3	2.3
		3	502.5	∞	65.6

Table A4. *Summary of VES Results Analysis along Profile E.*

VES point	Type of curve	No of layers	Average resistivity (Ωm)	Layer thickness (m)	Depth starting from (m)
		1	414.7	2.6	0.0
E_1	H	2	98.6	26.1	2.6
		3	5372.8	∞	28.7
		1	888.9	3.5	0.0
E_2	H	2	36.0	7.0	3.5
		3	3998.2	∞	10.5
		1	147.5	0.7	0.0
E_3	H	2	39.5	6.0	0.7
		3	1625.8	∞	6.7
		1	426.2	1.1	0.0
E_4	H	2	69.2	11.3	1.1
		3	687.6	∞	12.4
		1	966.9	1.4	0.0
E_5	H	2	18.4	4.1	1.4
		3	813.7	∞	5.5
		1	1331.6	1.5	0.0
E_6	H	2	244.9	44.0	1.5
		3	911.1	∞	45.5

Figures A1-A6: Iso-Resistivity maps for surface, 5 m, 10 m, 15 m, 20 m and 30 m.

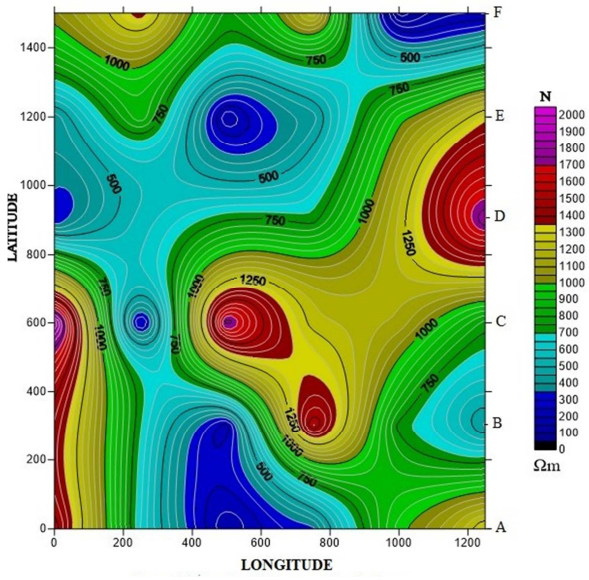

Figure A1. *Iso-Resistivity maps for surface.*

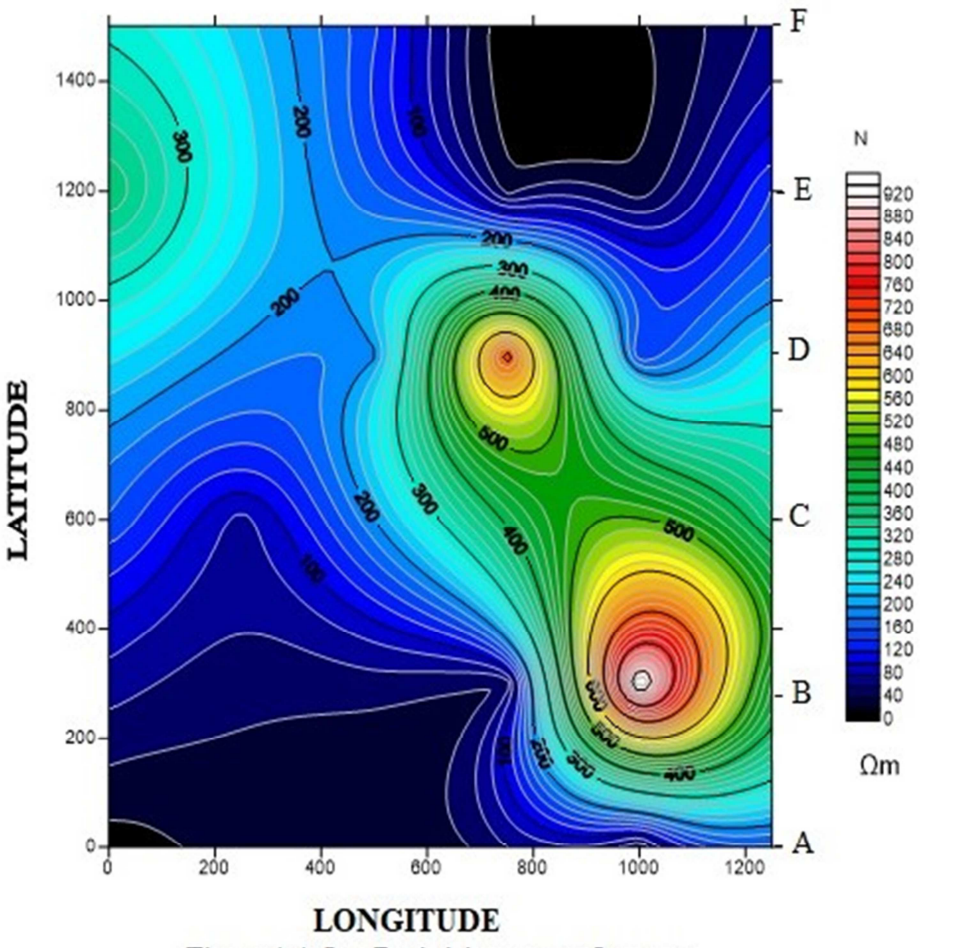

Figure A2. *Iso-Resistivity maps for 5 m depth.*

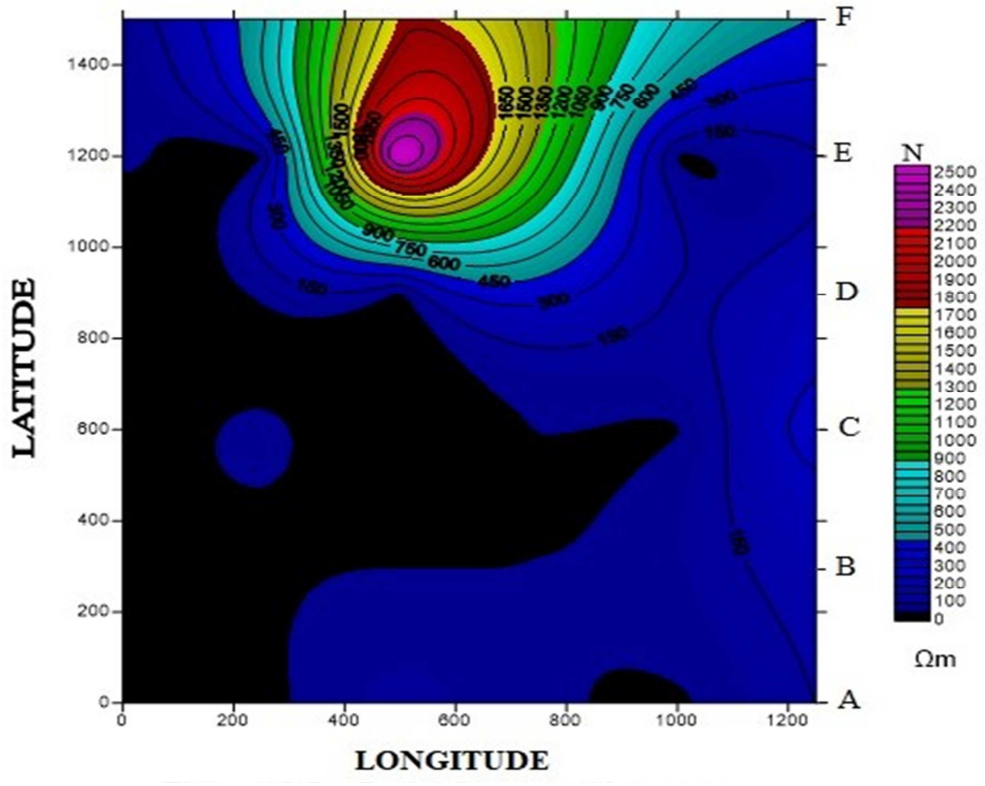

Figure A3. *Iso-Resistivity maps for 10 m depth.*

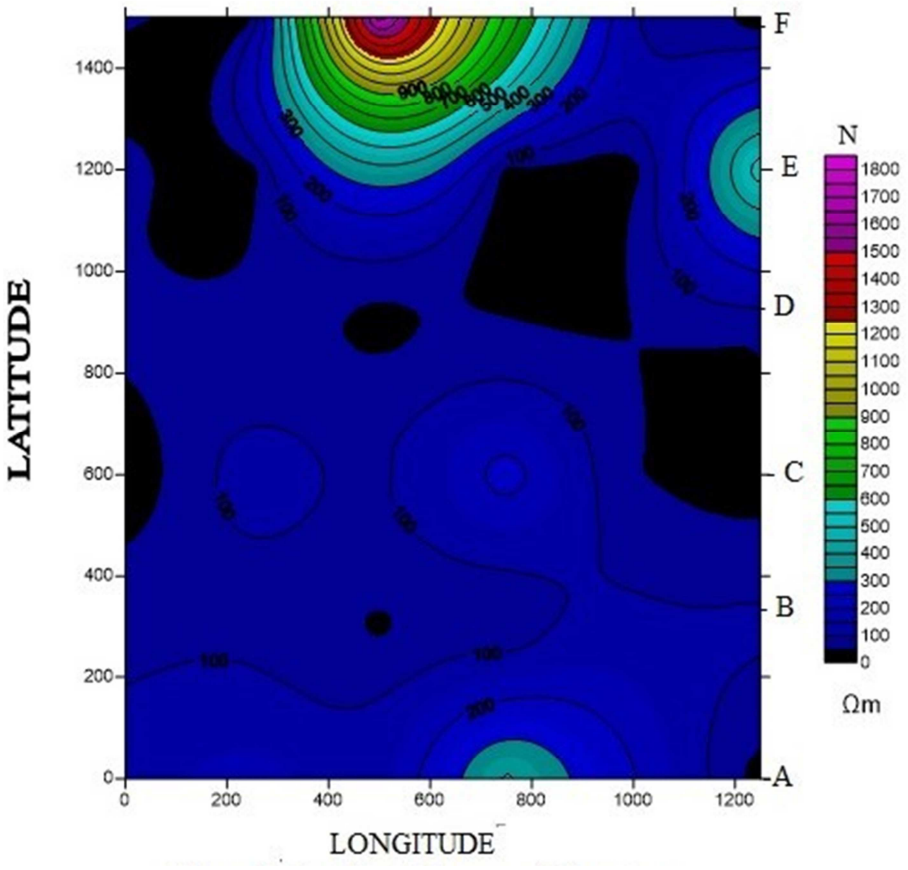

Figure A4. *Iso-Resistivity maps for 15 m depth.*

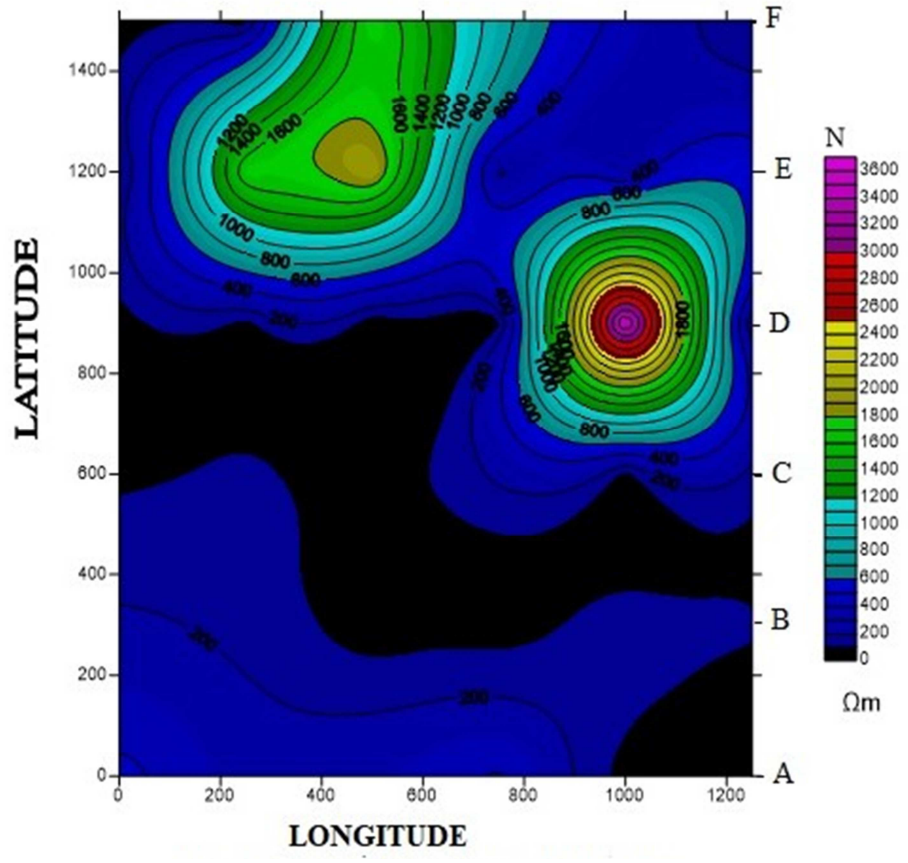

Figure A5. *Iso-Resistivity maps for 20 m depth.*

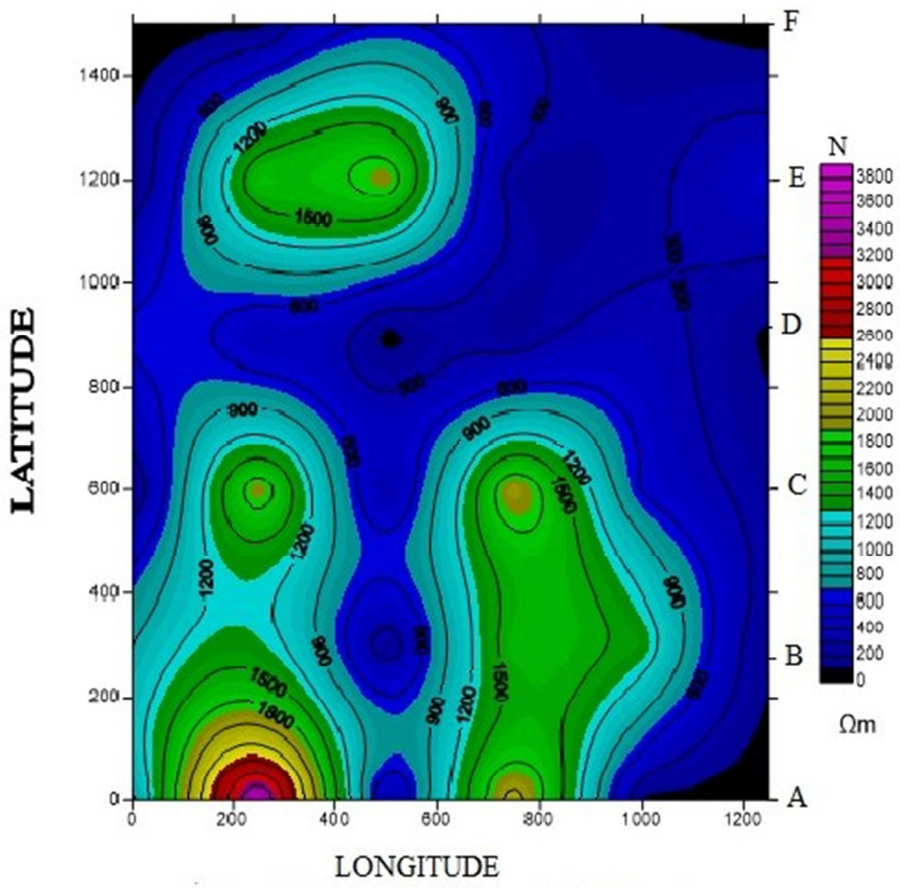

Figure A6. *Iso-Resistivity maps for 30 m depth.*

References

[1] Abdullahi, N. K. and Iheakanwa, A. 2013. Groundwater detection in basement complex Northwestern Nigeria using 2D electrical resistivity and offset wenner techniques. *International Journal of Science and Technology*, 2 (5): 529-535.

[2] Abiola, O., Enikanselu, P. A., & Oladapo, M. I. (2009). Groundwater potential and aquifer protective capacity of overburden units in Ado-Ekiti, Nigeria. *International Journal of Physical Sciences* 4 (3): 120–132.

[3] Adetona, A. A., Salako, K. A., Abdulrashid, U. A., Rafiu, A. A., Ofor, N. P., Alhassan, D. U., & Jonah, S. A. (2013). Geophysical Investigation of Western Part of Federal University of Technology, Gidan Kwano Campus, Minna, Niger State, Using Electrical and Seismic Refraction Methods. *Natural and Applied Sciences Journal:* 11 (2).

[4] Ajayi, C. O., & Hassan, M. (1990). The delineation of the aquifer overlying the basement complex in western part of the Kubanni Basin of Zaria (Nigeria). Journal of Mining and Geology, 26 (1), 117-124.

[5] Ajayi, C. O & Anthony, C. W. (1988). Groundwater prospects in the basement complex rock of southwestern Nigeria. *Journal of African Earth Sciences,* 7 (1): 227–235.

[6] Ajibade, A. C. (1980). The geology of the country around Zungeru, Northwestern state of Nigeria. Unpublished M. Sc. thesis, University of Ibadan, Ibadan, Nigeria.

[7] Alagbe O A, Sunmonu L A, Adabanija M A (2013), Res. Journal of Physical Sciences, 1 (3), 1-5.

[8] Alhassan, D. U., Mohammed, I. N., Bature, M., Kimpe, M. I., & Mohammed, A. (2015). Electrical resistivity survey for groundwater at Eye Zheba village. Off Bida- Minna road. *Journal of Applied Geology and Geophysics,* 3 (2): 49–53.

[9] Alhassan, D. U., Obiora, D. N., & Okeke F. N. (2017). Geoelectrical investigation of groundwater potentials of northern Paiko, Niger state, northcentral Nigeria. *Journal of Earth Science,* 28 (1): 103–112.

[10] Atakpo, E. A. and Ayolabi, E. A. (2009). Evaluation of Aquifer vulnerability and the protective capacity in some oil producing communities of western Niger Delta. *Journal of Environmentalist*, 29 (3): 318–322.

[11] Balasubramanian, A. (2017). Methods of Groundwater exploration. Centre for advanced studies in earth science, University of Mysore. Mysore-6 publications.

[12] Benson, A. K., Payne, K. L., & Stubben, M. A. (1997). Mapping groundwater contamination using dc resistivity and VLF geophysical methods; a case study. Geophysics, 62 (1), 80-86.

[13] Chambers, J. E., Kuras, O., Meldrum, P. I., Ogilvy, R. D., & Hollands, J. (2006). Electrical resistivity tomography applied to geologic, hydrogeologic, and engineering investigations at a former waste-disposal site. Geophysics, 71 (6), B231-B239.

[14] Dobrin, M. B., & Savit, C. H. (1960). Introduction to geophysical prospecting (Vol. 4). New York: McGraw-hill.

[15] Ebong, E. D., Akpan, A. E., & Onwuegbuche, A. A. (2014). Estimation of geohydraulic parameters from fractured shales and sandstone aquifers of Abi (Nigeria) using electrical resistivity and hydrogeologic measurements. Journal of African Earth Sciences, 96, 99-109.

[16] Grant, F. S., & West, G. F. (1965). Interpretation theory in applied geophysics. New York: McGraw-Hill.

[17] Isaac, O. A., Ezikiel, A., Isaac, I. M., Jacob, B. J., Peace, E. A., Goodness, E. J., Nurudeen, R., & Peace N. J. (2022). Aquifer vulnerability and protective cacacity test of Lokoja, Kogi state, Nigeria. *International Journal of Applied Chemical and Biological Sciences* 3 (4): 41–48.

[18] Levi, I. N. (2011). 2D Resistivity Survey for Ground water Exploration in a Hard Rock Terrain: A Case Study of MAGDAS Observatory, Unilorin, Nigeria. *Asian Journal of Earth Sciences* 4 (1): 46-53Lowerie, W. (1997). Fundamental of geophysics, electromagnetic surveying Cambridge University press. P. 220–223.

[19] McCurry, P. (1976). The geology of the Precambrian to lower Paleozoic rocks of northern Nigeria, a review inc A, Kagbe (ed), geology of Nigeria, 15 – 39. Lagos, Elizabethan publishing co.

[20] Mosuro, G. O., Omosanya, K. O., Bayewu, O. O., and Oloruntola, M. O. (2017). Assessment of groundwater vulnerability to leachate infiltration using electrical resistivity method. *Journal of applied Water Sciences* 7: 2195–2207. https://doi.org/10.1007/s1320 1-016-0393-4.

[21] Ogungbemi, O. S., Badmus Ganiyu, O., Idowu, K. A., & Oluwatoyin, O. (2013). Geoelectric and electromagnetic methods for post foundation studies in a typical basement terrain. Journal of Emerging Trends in Engineering and Applied Sciences, 4 (6), 863-868.

[22] Oladapo, M. I. and Akintorinwa, O. J. (2007). Hydrogeophysical study of Ogbese Southwestern, Nigeria. *Global Journal of. Pure and Applied Sciences.* 131: 55-61.

[23] Olorunfemi, M. O. & Fasuyi, S. A. (1993). Aquifer types and geoelectric/hydrogeologic characteristics of part of central basement terrain of Nigeria, (Niger state). *Journal of African Earth Sciences.* 16 (3): 157–160.

[24] Olorunfemi, M. O., Ojo, J. S., & Akintunde, O. M. (1999). "Hydrogeophysical evaluation of the groundwater potential of Akure metropolis, southwestern Nigeria". *Journal of Mining and Geology.* 35 (2): 207–228.

[25] Oluwafemi, O., & Oladunjoye, M. A. (2013). Integration of surface electrical and electromagnetic prospecting methods for mapping overburden structures in Akungba-Akoko, Southwestern Nigeria. International Journal of Science and Technology, 2 (1), 122-147.

[26] Onyenweife, G. I., Nwozor, K. K., Nwike, I. S., Onuba, L. N., Egbunike, M. E. & Anakor, S. N (2020). Application of electrical resistivity method in estimating aquifer protective capacity of Akwa and its environs, Anambra state, Nigeria. *International Journal of Innovative Environmental Studies Research,* 8 (4): 1–17.

[27] Oseji, J. O., Atakpo, E. A. & Okolie, E. C. (2005). Geoelectric investigation of the aquifer characteristics and groundwater potential in Kwale, Delta state, *Nigeria. Journal of Applied Sciences and Environmental Management.* 9: 157-160.

[28] Parasnis, D. S. (1987). *Principle of Applied Geophysics*. London: Chapman and Hall Ltd.

[29] Perez, J. W., & Barber, M. (1965). Distribution and chemical quality of groundwater in northern Nigeria. *Geological Survey of Nigeria Bulletin,* 36.

[30] Salako, K. A., Adetona, A. A., Rafiu, A. A., Ofor, N. P., Alhassan, U. D., & Udensi, E. E. (2009). Vertical electrical sounding investigation for groundwater at the southwestern part (site A) of Nigeria Mobile Police barracks (MOPOL 12), David Mark road, Maitumbi, Minna. *Journal of Science, Education and Technology*, 2: 350–362.

[31] Sharma S. P. & Baranwal, V. C. (2005) Journal of Applied Geophysics, 37, 155-166.

[32] Sunmonu L A, Alagbe O A, (2011) Internal Journal of Physics, 3 (1), 70-75.

[33] Sunmonu, L. A., Adagunodo, T. A., Olafisoye, E. R. & Oladejo, O. P. (2012). The groundwater potential evaluation at industrial estate Ogbomosho southwestern Nigeria. *RMZ-Materials and Geoenvironment,* 59 (4): 363–390.

[34] Sunmonu, L. A., Adagunodo, T. A., Adeniji, A. A., Oladejo, O. P. & Alagbe O. A. (2015). Geoelectric delineation of aquifer pattern in crystalline bedrock. *Open Transactions on Geosciences.* 2 (1): 1–16.

[35] Sunmonu, L. A., Adagunodo, T. A., Bayowa, O. G. & Erinle, A. V. (2016). Geophysical mapping of the proposed Osun state housing estate, Olupona for subsurface competence and groundwater potential. *Journal of Basic and Applied Research.* 2 (2): 27–47.

[36] Telford, W. M., Geldart, L. P., Sheriff P. E., & Keys, D. A. (1976). Applied Geophysics. Cambridge: Cambridge University Press. Pp 1-5, 630-640.

[37] Telford, N., Geldert, L. P., Sheriff, R. S., & Keys, D. A. (1990). *Applied Geophysics*, 2nd edition. Cambridge, University Press.

[38] Tsepav, M. T., & Umar, M. A. (2016). Evaluation of aquifer protective capacity and soil corrosivity using geoelectrical method. *World Engineering and Applied Sciences Journal* 7 (3): 135-144.

[39] Udensi, E. E., Ogunbanjo, M. I., Nwosu, J. E., Jonah S. A., Kolo, M. T., Onuduku, U. S., Crown, I. E., Daniyan, M. A., Adeniyi, J. O. & Okosun, F. A. (2005). Hydrogeological and Geophysical surveys for groundwater at designated premises of the main Campus of the Federal University of Technology, Minna. Zuma Journals of Pure and Applied Science (ZJ PAS). 7 (1) pp. 52-58.

[40] UNESCO, (2007). Record of illness and death from Water related diseases in the developing countries. *Journal of Medical Ethics* 33 (3): 150–154.

[41] United Nations Educational, Scientific, and Cultural Organization. World Water Balance and Water Resources of the Earth. 1996.

[42] Yadav, G. S., & Singh, S. K. (2007). Integrated resistivity surveys for delineation of fractures for ground water exploration in hard rock areas. Journal of applied geophysics, 62 (3), 301-312.

[43] Henriet, J. P. (1976). Direct applications of the Dar Zarrouk parameters in ground water surveys. *Geophysical prospecting*, *24* (2), 344-353.

[44] Dan-Hassan, M. A., & Olarinfemi, M. O (2015). Hydro-geophysical investigation of a basement terrain in the North-Central part of Kaduna State, Nigeria. Journal of Mining & Geology, 35 (2), 189–206.

[45] AB, A. I. (1999). ABEM Terrameter SAS 4000/SAS 1000 Instrument Manual. *ABEM Printed Matter*, (93101).